Available online at www.sciencedirect.com
SCIENCE DIRECT
Thermochimica Acta 440 (2006) 111–121
thermochimica acta
www.elsevier.com/locate/tca

Thermal and crystallization studies of short flax fibre reinforced polypropylene matrix composites: Effect of treatments

A. Arbelaiz, B. Fernández, J.A. Ramos, I. Mondragon *

"Materials + Technologies" Group, Dpto. Ingeniería Química y M. Ambiente, Escuela Univ. Politécnica, Euskal Herriko Unibertsitatea/Universidad del País Vasco, Plaza Europa 1, 20018 Donostia-San Sebastián, Spain

Received 19 July 2005; received in revised form 15 September 2005; accepted 21 October 2005
Available online 29 November 2005

Abstract

The effect of fibre treatments on thermal stability of flax fibre and crystallization of flax fibre/polypropylene composites was investigated. For thermal stability study, flax fibres have been treated using maleic anhydride, maleic anhydride polypropylene copolymer, vinyltrimethoxy silane and alkalization. In order to compare thermal stability of flax fibres thermogravimetry (TG) analysis has been used. Kinetic parameters have been determined by Kissinger method. Results showed that all treatments improved thermal stability of flax fibres. For crystallinity analysis, three different techniques have been used, differential scanning calorimetry analysis (DSC), pressure–volume–temperature (PVT) measurements for analysis of volume shrinkage and polarized optical microscopy (POM). All techniques results showed that addition of flax fibre increased crystallization rate. Besides, depending on fibre surface treatment and crystallization temperature, flax fibre/PP composites can show transcrystallinity.

Keywords: Flax fibre; Polypropylene; Thermal stability; Crystallinity; Transcrystallization

1. Introduction

There is an increasing interest in using natural fibres as reinforcing agents in composites because they have a number of advantages as they combine good mechanical properties with renewability and biodegradability [1–3]. However, the main disadvantage of natural fibres is their hydrophilic nature that lowers the compatibility with hydrophobic polymeric matrices during composite fabrication [3]. In the literature survey [4–9] different surface treatments have been used to improve lignocellulosic fibre/polypropylene adhesion in natural fibre composites. The application of surface treatments could affect the thermal stability of natural fibres. On the other hand, lignocellulosic fibres are submitted to intense heat during composite fabrication. Therefore, thermal analysis study is necessary to determine the influence of surface treatments on thermal stability of natural fibres and also to observe any degradation process during composites production. Most properties of semicrystalline thermoplastic polymeric composites materials are a complex function of a number of parameters such as mechanical properties, shape, size, orientation and distribution of the reinforcement and the mechanical properties of the matrix. Mechanical properties of the matrix are affected by a number of variables including degree of crystallinity, size and number of spherulites [10]. Addition of filler in PP matrix can affect its crystallization. Besides, mechanical properties of composites are greatly dependent on the crystalline structure affected by the filler [11]. In a previous work [12], the effects of surface modification on tensile properties of single fibres, fibres wettability and fibre–matrix interfacial shear strength were reported. In this paper, thermal stability and kinetic parameters for thermal degradation of untreated and treated flax fibres have been analyzed. Kinetic parameters have been determined by the Kissinger method. On the other hand, crystallization of neat PP and flax fibre/PP composites under quiescent state has been analyzed. The effect of nucleating ability of untreated and treated flax fibre on PP has also been investigated.

2. Approach to thermal stability analysis

Thermogravimetric data can be analyzed using kinetic parameters. For many degradation processes, the rate of reaction

* Corresponding author. Tel.: +34 94 3017177; fax: +34 94 3017130.
E-mail address: iapmoegi@sc.ehu.es (I. Mondragon).

0040-6031/$ – see front matter © 2005 Elsevier B.V. All rights reserved.
doi:10.1016/j.tca.2005.10.016

can be expressed as follows:

$$\frac{d\alpha}{dt} = k(T) f(\alpha) \quad (1)$$

where t is reaction time, α the conversion degree and $k(T)$ is the reaction rate constant.

Conversion can be defined as [13],

$$\alpha = \frac{w_o - w}{w_o - w_\infty} \quad (2)$$

where w, w_o and w_∞ are the mass at t, 0 and at the termination times, respectively.

k, the constant of the rate of reaction, is generally expressed by Arrhenius equation as,

$$k(T) = A \exp\left(-\frac{E}{RT}\right) \quad (3)$$

where A is the pre-exponential factor (1/min), E the apparent activation energy (J/mol), T the absolute temperature (K) and R is the gas constant (8.3136 J/mol K).

Combining Eqs. (1) and (3), it results in the following equation:

$$\frac{d\alpha}{dt} = A \exp\left(-\frac{E}{RT}\right) f(\alpha) \quad (4)$$

where $f(\alpha)$ is the kinetic function which depends on the reaction model [14,15]. Its definition is normally very complicated because many reactive processes may occur simultaneously [16]. The simplest model used to describe the kinetic function $f(\alpha)$ is the following [13]:

$$f(\alpha) = (1 - \alpha)^n \quad (5)$$

where n is reaction order.

Taken into account that β is the heating rate used in thermogravimetric analysis ($\beta = dT/dt$)

$$\frac{d\alpha}{dT} = \frac{A}{\beta} \exp\left(-\frac{E}{RT}\right)(1 - \alpha)^n \quad (6)$$

Kissinger method [17] supposes a first-order kinetic ($n = 1$). This method allows the calculation of E from a point T_{max}, being T_{max} the temperature at the maximum of the derivative thermogravimetric curve (DTG),

$$\left(\frac{d^2\alpha}{dT^2}\right)_{max} = 0 = \frac{A}{\beta}\left(\frac{E}{RT_{max}^2}(1 - \alpha)^n + n(1 - \alpha)^{n-1}\left(-\frac{d\alpha}{dT_{max}}\right)\right) \exp\left(-\frac{E}{RT_{max}}\right) \quad (7)$$

$$\ln\left(\frac{\beta}{T_{max}^2}\right) = -\ln\left(\frac{E}{AR}\right) - \frac{E}{R}\left(\frac{1}{T_{max}}\right) \quad (8)$$

Plotting $\ln(\beta/T_{max}^2)$ against $(1/T_{max})$ the slope of straight line is $-E/R$.

For each degradation step a sudden mass loss was observed and the activation energy can thus be calculated [17]. However, we have focused our attention on the second mass loss which is flax fibre main degradation step.

3. Experimental

3.1. Materials

A commercially available polypropylene "Eltex-P HV200" produced by Solvay with a melt flow index of 10 g/10 min (at 230 °C and 2.16 kg) was used as polymeric matrix. Retted flax fibre bundles kindly supplied by Finflax Company (Finland) were used. As compatibilizers Epolene E43 (maleic anhydride–polypropylene copolymer) produced by Eastman Chemical, maleic anhydride (MA) obtained from Cepsa Company and vinyltrimethoxy silane (VTMO) kindly supplied by Degussa-Hüls were used. Epolene E43 has a low molecular weight (M_n = 3900 and M_w = 9100), 0.934 g/mL density and acid number of 45 [18]. On the other hand, alkalization was carried out using NaOH pellets. Fibres were treated with 10 wt% of MA. Fibres were esterified for 25 h with MA and dissolved in boiling acetone ($T = 50 \pm 5$ °C) with a fibre/solvent ratio of 1:25 (w/v). Thereafter, fibres were washed several times in cold acetone and distilled water, and finally dried in an oven at 105 °C [19]. Treatment with 10 wt% MAPP was also used. For this treatment, MAPP was dissolved in boiling xylene ($T = 150 \pm 5$ °C) with a fibre/solvent ratio of 1:25 (w/v). Then, the fibres were soaked in the solution for 5–6 min. As in the former case, the fibres were washed and carefully dried [19,20]. For silanization, VTMO was dissolved in acidified water (pH 3.5) for 10 min to get a better functionalization. Then, the fibres were added and maintained for 1 h in the solution to obtain a 2.5 wt% [21]. Alkalization consisted in soaking the fibre in a 20 wt% aqueous solution of sodium hydroxide for 1 h at room temperature. Afterwards, the alkalized fibre was washed for several times in distilled water followed by neutralization with a few drops of acetic acid. Fibres were then washed again and finally dried in an oven. The ratio of fibre weight to alkali solution volume corresponded to 1:20 [22].

3.2. Composites fabrication

For crystallinity analysis with DSC and PVT techniques, 30 wt% flax fibre bundle composites were fabricated. Flax fibre bundles were first chopped to a length of approximately 30 mm and the diameter values varied from 10 to 120 μm. Prior to mixing, fibres were dried in a vacuum oven at 100 °C for 12 h.

Compounding of the materials was carried out using an internal mixer (Haake Rheomix 600 with two Banbury rotors). The mixing temperature was set at 180 °C and after loading all components, they were mixed for 5 min at 40 rpm. The mixture was pelletized and kept in a vacuum oven at 100 °C for 12 h. Moulding of the dried pellets was carried out in an injection-moulding machine (Battenfeld Plus 250). DSC and PVT measurements have been carried out with small pieces cut from moulded composites.

3.3. Thermogravimetry analysis (TGA)

In order to study thermal stability of untreated and treated fibres, thermogravimetric analysis has been carried out using a Setaram 92-12 thermoanalyzer. Samples weighing between 10 and 20 mg were placed in ceramic crucibles and tests were carried out in helium atmosphere between 30 and 800 °C. Different scan rates were used, 5, 10, 15 and 20 °C/min.

3.4. Differential scanning calorimetry analysis (DSC)

DSC measurements were performed using a differential scanning calorimeter (DSC 822e, equipped with an intracooler, Mettler Toledo). Temperature calibration and determination of the constant time of the instrument were performed by using standards of In and Zn, and the heat flow calibration with In. Isothermal and dynamic scans were carried out in nitrogen atmosphere.

3.4.1. Isothermal measurements

Samples between 5 and 10 mg were heated to 200 °C and the melt was held 5 min to erase the thermal history of the polymer. Then, samples were cooled at two different cooling rates (5 and 20 °C/min) to a given crystallization temperature (T_c). Isothermal crystallizations were carried out at different temperatures, 134, 140 and 145 °C, to analyze the effects on the crystallization kinetics. The results were analyzed using Avrami theory.

3.4.2. Dynamic measurements

For dynamic testing, previously isothermally obtained samples were used which were heated from 25 to 200 °C at a rate of 10 °C/min.

3.5. Pressure–volume–temperature measurements (PVT)

A pressure–volume–temperature analyzer (SWO/Haake PVT 100) was used to measure the volumetric shrinkage during crystallization process. Several isotherms (134, 140 and 145 °C) under 200 bar pressure were carried out to measure specific volume variations along the time. Samples between 0.6 and 1 g were heated to 200 °C and melt was held 5 min to erase the thermal history of the polymer. Then, 400 bar pressure was applied to release bubbles and samples were cooled at 10 °C/min cooling rate under 200 bar to a given crystallization temperature (T_c) where crystallization was allowed to occur until completion. Isothermal crystallizations were carried out at temperatures selected in DSC measurements. Results were also treated with Avrami theory.

3.6. Polarized optical microscopy (POM): crystallinity

Nucleation studies were carried out by using a Nikon Eclipse E600W polarized optical microscope equipped with a Mettler hot stage (model FP82HT). Photomicrographs of growing spherulites and transcrystalline layer were taken at time intervals to evaluate the growth of both spherulites and transcrystalline layer.

Single fibre-embedded PP film samples were prepared by placing an untreated or treated fibre on the molten PP covering them with a cover slip. The system was heated above the melting temperature of PP and maintained at 200 °C for 5 min to erase the previous thermal history. Then, samples were cooled at a rate of 10 °C/min to different crystallization temperatures (134, 140 and 145 °C).

4. Results and discussion

4.1. TG measurements

Thermogravimetry (TG) and DTG curves for untreated flax fibre bundles obtained in helium at different heating rates are shown in Fig. 1. Three weight loss stages can be seen, which is in agreement with other lignocellulosic fibre studies [23–25]. For all samples studied, the first weight loss observed is attributed to the evaporation of water. Table 1 shows that treated flax fibres became more hydrophobic after treatments as the amount of water weight loss decreased. The arithmetic mean from all heating rates was used to obtain values for moisture level. About 8–40% reduction in the moisture content was observed as a function of the treatment used. It is evident that untreated and treated flax fibres contain a significant level of water, which is released when flax fibre/polypropylene composites are produced, confirming the need to pre-dry these fibres prior to processing, or to employ devolatilization procedures during compounding to remove evolved steam [26]. The second peak is related to the degradation of cellulose, hemicelluloses and pectins [27,28]. Except for silane and alkali treated fibres, all fibres DTG curves show a shoulder between 250 and 350 °C (Fig. 1a) which corresponds with the pectins and hemicelluloses content [28]. Alkali treatment removes pectins and hemicelluloses which degrade at lower temperature, thereby the peak of DTG did not show a shoulder after fibre alkalization. For VTMO treatment, the absence of shoulder could be explained by the thermal stability improvement of hemicelluloses and pectins. For sisal fibres, Joseph et al. [23] suggested that the third peak, between 450 and

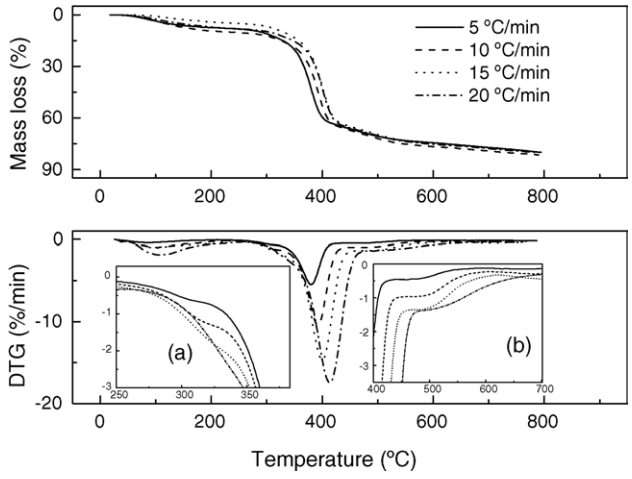

Fig. 1. TG and DTG thermograms of untreated flax fibres at different heating rates. Magnified view in the temperature range of: (a) 250–380 °C and (b) 400–700 °C.

Table 1
The first peak mass loss percentages and kinetic parameters calculated from Kissinger equation for thermal degradation of untreated and treated flax fibres

Treatment	Mass loss, % (T_{peak}, °C)					Kinetic parameters	
	5 °C/min	10 °C/min	15 °C/min	20 °C/min	Mean value	ln A	E (kJ/mol)
Untreated	8.01 (87)	10.1 (102)	7.94 (128)	10.0 (107)	9.02	23.8	138
VTMO	4.37 (80)	7.18 (104)	3.96 (111)	6.05 (108)	5.39	17.3	169
MA	4.21 (88)	5.91 (94)	4.90 (104)	7.40 (97)	5.60	24.3	140
MAPP	4.90 (76)	6.50 (78)	5.93 (99)	6.71 (104)	6.01	26.9	154
NaOH	8.34 (87)	8.92 (95)	6.98 (109)	9.31 (108)	8.39	27.2	159

550 °C (Fig. 1b), might be due to the further breakage of decomposition products of fibres. At 350 °C, the formation of aromatic compounds starts, and between 400 and 500 °C, they constitute 88% of the ash. Ash produced by pure cellulose consists mainly of polycyclic aromatic compounds [24]. All fibres have a residual weight between 17 and 24 wt% at 750 °C. Devallencourt et al. [29] observed residual weight about 17% for cellulose ashless filter paper after heating from 20 to 900 °C. In an inert atmosphere, the end-products of the degradation of cellulose are carbonaceous residues plus undegraded fillers, when they exist [29]. As during flax plant growing, plant needs inorganic compounds as nutrients, these inorganic compounds will show up in the ash [24].

Thermogravimetric data can also be analyzed using kinetics parameters such as activation energy and pre-exponential factor. Table 1 shows the kinetic parameters calculated from Kissinger equation for degradation of untreated and treated flax fibres in helium flow. E values obtained by Devallencourt et al. [29] for different cellulose samples using Kissinger's method are in the range of 173–177 kJ/mol. On the other hand, Van de Velde and Kiekens [24] reported that the activation energy of flax fibre ranges between 92.4 and 181.7 kJ/mol in nitrogen atmosphere using Broido formula. So that, our values are of the same order of magnitude as for cellulosic fibres reported in literature survey. All treated fibres showed higher E values than those of untreated flax fibre ones resulting in thermal stability improvement since a higher value of E points to a more stable substance. Similar trends were observed by other authors for other lignocellulosic fibres [25,27]. Zafeiropoulos et al. [1] found that acetylation and stearic acid treatment of flax fibres improved their thermal stability. Therefore, all surface treatments improved in some extent flax fibre thermal stability. Taking into account that only MAPP treatment increases both tensile strength of flax fibre and flax fibre/PP adhesion as reported in a previous paper [12], crystallinity study of short flax fibre reinforced polypropylene matrix composites has been performed for MAPP-treated fibre and for comparison purpose untreated fibre and neat polypropylene have been used.

4.2. DSC measurements

Fig. 2 shows the DSC thermograms for pure PP obtained in different isothermal processes. Several models have been proposed for the theoretical treatment of isothermal crystallization kinetics [30]. Avrami model is universally used to describe polymer crystallization kinetics under isothermal conditions. The basic isothermal expression which relates the change in crystallinity with time is:

$$X_r = 1 - \exp(-kt^n) \quad (9)$$

where X_r is the relative crystallinity, t the time, k the kinetic rate constant and n is the Avrami exponent which is a parameter depending on the geometry of the growing crystals and on the nucleation process [31]. Eq. (9) can be transformed into logarithmic form. Therefore, the values of n and k were calculated from the slope and the intercept, respectively, of the straight line obtained by plotting $\log(-\ln(1 - X_r))$ against $\log t$ [31]. Fig. 3 shows Avrami theoretical and experimental values correlation at $T_c = 134$ °C. A good agreement between experimental and theoretical values was observed for all samples. Besides, at the later stages of crystallization data deviated from the linearity. This deviation has been attributed to the occurrence of a secondary crystallization [30,32]. The obtained Avrami parameters, n, and the kinetic constant, k, are reported in Table 2. The interpretation of the kinetic data revealed some difficulties: e.g. the starting time of crystallization cannot always be precisely determined, the initial section of the crystallization isotherm is recorded inaccurately at low T_c and the value $X_{r\infty}$ (the relative crystallinity at infinitive time) cannot be exactly determined [33]. The observed values of Avrami exponent for PP vary from 2.34 to 2.89. In the literature survey for calorimetric measurements, the Avrami exponent varies between 1.9 and 3.56 [30,31,34] being the Avrami exponent values obtained in this work in the range of those reported in literature. Their fractional values would be considered representative of the nearest integral

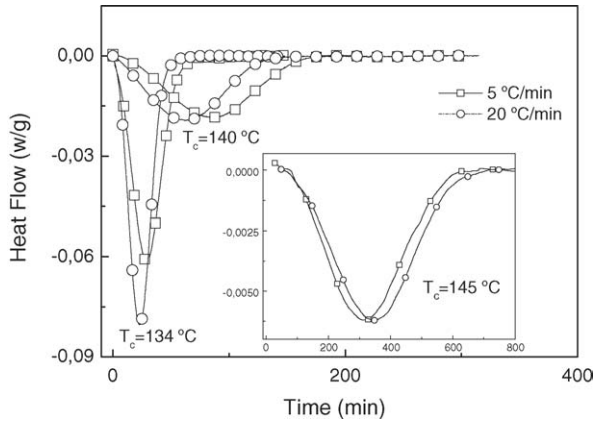

Fig. 2. DSC thermograms under different crystallization conditions for neat PP.

Table 2
Avrami parameters under different crystallization temperatures measured by DSC for neat PP, 30 wt% untreated flax + PP and 30 wt% MAPP-treated flax + PP

Sample	T_c	5 °C/min			20 °C/min		
		n	k (min^{-n})	$t_{1/2}$ (min)	n	k (min^{-n})	$t_{1/2}$ (min)
PP	134	2.51	1.47×10^{-4}	30.1	2.62	1.61×10^{-4}	24.2
	140	2.52	1.08×10^{-5}	81.6	2.34	4.46×10^{-5}	61.2
	145	2.34	1.53×10^{-6}	260	2.89	5.52×10^{-8}	288
30 wt% untreated flax + PP	134	2.31	1.28×10^{-3}	15.2	2.20	1.75×10^{-3}	15.2
	140	2.57	2.43×10^{-5}	54.2	2.28	7.79×10^{-5}	55.3
	145	2.64	1.31×10^{-6}	140	2.47	4.61×10^{-6}	126
30 wt% MAPP-treated flax + PP	134	2.40	7.36×10^{-3}	6.6	2.34	5.53×10^{-3}	7.8
	140	2.89	1.39×10^{-5}	40.2	2.49	6.48×10^{-5}	41.3
	145	2.74	1.66×10^{-6}	108	2.54	4.57×10^{-6}	110

values or an average contribution of simultaneous occurrence of various types of nucleation and growth of crystallization, each conforming to different integral values of the exponent n [35]. Crystallization rates of all systems are strongly influenced by the crystallization temperature. It is observed that increasing crystallization temperature involves a decrease of the crystallization rate. On the other hand, cooling rate did not have any significant effect on Avrami parameters.

After flax fibres addition crystallization process was faster probably due to the fibres acting as an efficient nucleating agent for the crystallization of PP and, consequently, increasing the crystallization rate of PP [36,37]. Besides, MAPP-treated flax fibre composite showed the fastest crystallization process. Lopez Manchado et al. [38] found for sisal fibre/PP/EPDM composites that Avrami exponent values obtained by DSC data varied between 2.20 and 2.96, similar to those obtained in this study.

Fig. 4 shows DSC heating scans of neat PP after crystallization process. Samples have been cooled from the melt to the crystallization temperature at 5 °C/min. These curves show single fusion endotherm with two shoulders. The position of the peak and shoulders varies depending on the isothermal conditions used. Multiple fusion endotherms of iPP are believed to be due to the recrystallization of originally formed imperfect crystals [35,39]. Thermal parameters as melting temperature (T_m), heat of fusion (ΔH_f) and percentage of crystallinity (X_c), determined from the fusion run after isothermal crystallization process, are summarized in Table 3. The values of T_m and ΔH_f were obtained from the maxima and the area of the melting peaks, respectively [40]. The degree of crystallinity, X_c, of samples was calculated as follows [10]:

$$X_c = \frac{\Delta H_f}{\Delta H_f^\circ} \tag{10}$$

being ΔH_f° the heat of fusion of a hypothetical 100% crystalline sample and ΔH_f° taken as 209 J/g [10,13,31].

It is clear from Table 3 that the addition of flax fibres to PP causes only a marginal effect on the T_m which is in agreement with results reported by Joseph et al. [23] for sisal/PP composites. However, they found that as a result of fibre surface modification by chemical treatments the compatibility between the fibre and PP matrix was increased favouring interaction between the fibre and PP, so resulting in T_m changes which is in contrast with the values reported in Table 3. Increasing crystallization temperature, melting temperature is increased. This behaviour could be explained by the formation of more perfect crystals during crystallization. After addition of flax fibres, the values of ΔH_f decrease because fibres act as a diluent in the PP matrix [41]. However, taking into account the mass fraction of

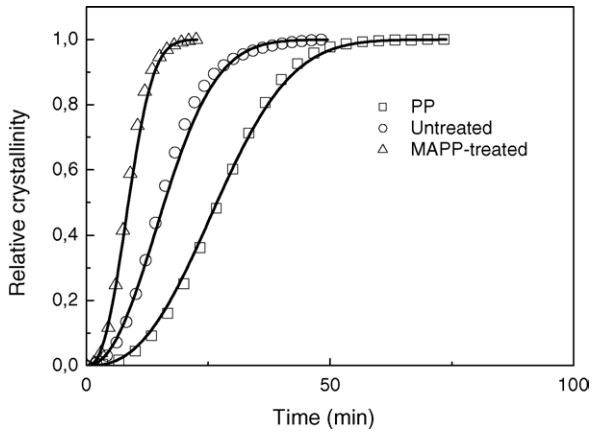

Fig. 3. Extent of relative crystallization of samples cooled at 10 °C/min and at T_c = 134 °C obtained by DSC, experimental values (open symbols) and theoretical values (line).

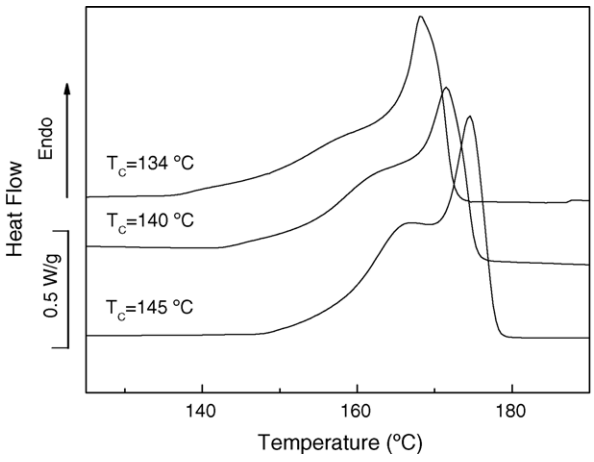

Fig. 4. DSC heating scans after crystallization at different temperatures for neat PP.

Table 3
Thermal parameters calculated from the fusion run after isothermal crystallization at several temperatures for neat PP, untreated and MAPP-treated flax fibre composites

Parameter	T_c = 134 °C			T_c = 140 °C			T_c = 145 °C		
	PP	Untreated	MAPP	PP	Untreated	MAPP	PP	Untreated	MAPP
T_m (°C)	168.4	167.7	167.8	171.5	171.0	170.5	174.6	174.4	173.9
H_f (J/$g_{composite}$)	104.3	74.8	67.4	104.9	78.6	68.0	119.9	76.8	79.9
H_f (J/g_{PP})	104.3	106.8	96.3	104.9	112.3	97.1	119.9	109.7	114.1
X_c (%)	49.9	51.1	46.1	50.2	53.7	46.5	57.4	52.5	54.9

PP in composites (0.7), and comparing X_c of neat PP with the percentage of crystallinity for the PP component in the composites, except for T_c = 145 °C, samples with untreated flax fibre showed higher crystallinity percent values than for unfilled PP. Therefore, below 145 °C untreated flax fibre surfaces seem to act as nucleation agent. However, when T_c = 145 °C, untreated flax fibre nucleation sites seem to be deactivated. For MAPP-treated fibre system, for all crystallization temperatures the crystalline index values obtained are lower than for neat PP. Although treated fibres have some active points, these points are not sufficient to increase crystallinity index.

4.3. PVT measurements

In order to analyze the effect of pressure on crystallinity rate PVT technique has been used. Fig. 5 shows the variation of specific volume for neat PP obtained in isothermal processes under 200 bar pressure. During crystallization the specific volume decreases rapidly due to the lower specific volume of the crystalline regions [42]. The following expression relates the change in crystallinity as a function of specific volume [43]:

$$X_r = \frac{v_t - v_o}{v_\infty - v_o} \quad (11)$$

where v_t, v_o and v_∞ are the specific volumes at t, 0 and at the termination times, respectively. As can be seen, after crystallization the specific volume does not change any longer. Avrami equation can be used to analyze the crystallization kinetics of polymers, both at atmospheric and higher pressures [44]. Fig. 6 shows Avrami theoretical and experimental values of relative crystallinity upon time for different samples. As for DSC measurements, good agreement between experimental and theoretical values was observed for all systems. The obtained Avrami parameters, n, and the kinetic constant, k, are reported in Table 4. The observed values of Avrami exponent vary from 1.17 to 1.54. Therefore, the values obtained by the PVT technique are lower than for previously reported DSC values. The value of the Avrami exponent depends on the applied experimental method [45]. He and Zoller [46] found that for pressurized dilatometry measurements, the Avrami exponent of isotactic polypropylene varied between 1.3 and 1.7 (134–191 °C). So that, our values are close to those reported values. However, Watanabe et al. [44] found that for PP under various pressures in static condition, the Avrami exponent value of 3 gave the best fit to experimental data. Crystallization rates obtained under 200 bar pressure are higher than those obtained by DSC under atmosphere pressure as crystallization was accelerated by pressure. As for DSC values, the addition of flax fibres increased crystallization rate probably, as mentioned above, due to the fibres acting as an efficient nucleating agent for the crystallization of PP. The fastest system is MAPP-treated fibre/PP composites followed by untreated flax composites, being the slowest one neat PP system. The same order was also obtained in DSC measurements.

4.4. Polarized optical microscopy

In order to study morphology, micrographs have been analyzed by POM. Zafeiropoulos et al. [47] studied the effect

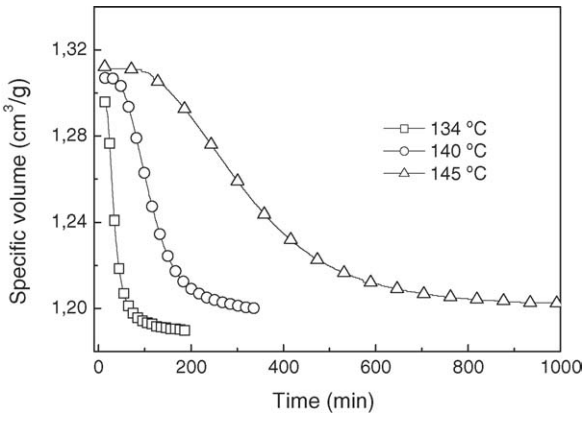

Fig. 5. Variation of specific volume under 200 bar pressure at different crystallization temperatures for neat PP.

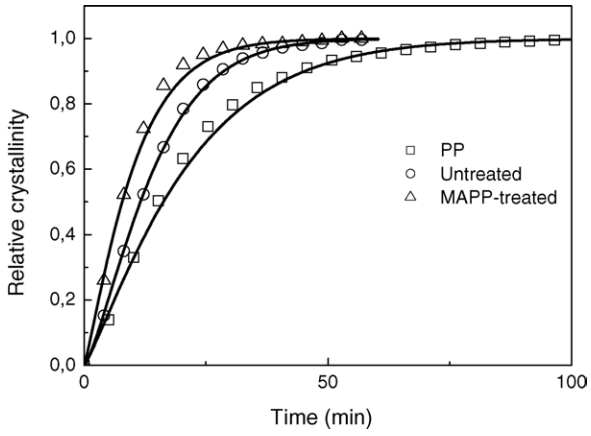

Fig. 6. Extent of relative crystallization of samples under different crystallization temperatures obtained by PVT, experimental values (open symbols) and theoretical values (line).

Table 4
Avrami parameters under different crystallization temperatures as measured by PVT for neat PP, untreated flax/PP composites and MAPP-treated flax/PP composites

T_c	PP			30 wt% untreated flax + PP			30 wt% MAPP-treated flax + PP		
	n	k (min^{-n})	$t_{1/2}$ (min)	n	k (min^{-n})	$t_{1/2}$ (min)	n	k (min^{-n})	$t_{1/2}$ (min)
134	1.17	2.63×10^{-2}	16.2	1.32	2.70×10^{-2}	11.5	1.17	6.30×10^{-2}	7.8
140	1.37	2.56×10^{-3}	59.2	1.38	4.09×10^{-3}	41.0	1.54	3.14×10^{-3}	33.2
145	1.31	6.88×10^{-4}	194.4	1.33	1.54×10^{-4}	97.8	1.43	1.05×10^{-4}	92.1

of different cooling rates from the starting to the crystallization temperature on transcrystallinity of flax fibre/PP composite materials. They found that the cooling rates did not have any significant effect upon transcrystallinity. Therefore, and also taking into account DSC results, POM study has been carried out only at one cooling rate (10 °C/min).

In general, polymer crystallization can be divided into two stages. The first stage (primary crystallization) is associated with the growth of spherulites which starts when a small stable crystal (nucleus) has formed in the melt. The crystalline lamellae grow radially outwards from this nucleus and by successive branching form the typical spherulite structure. When the spherulites impinge onto each other spherulite growth stops and the second stage starts. The secondary crystallization occurs more slowly being associated with material trapped within or between the spherulites [42,48].

Transcrystalline morphology is characterized by a dense heterogeneous nucleation of the matrix crystals at the fibre surface which grow perpendicular to the fibre axis, since neighbouring nuclei will hinder the lateral extension [49,50].

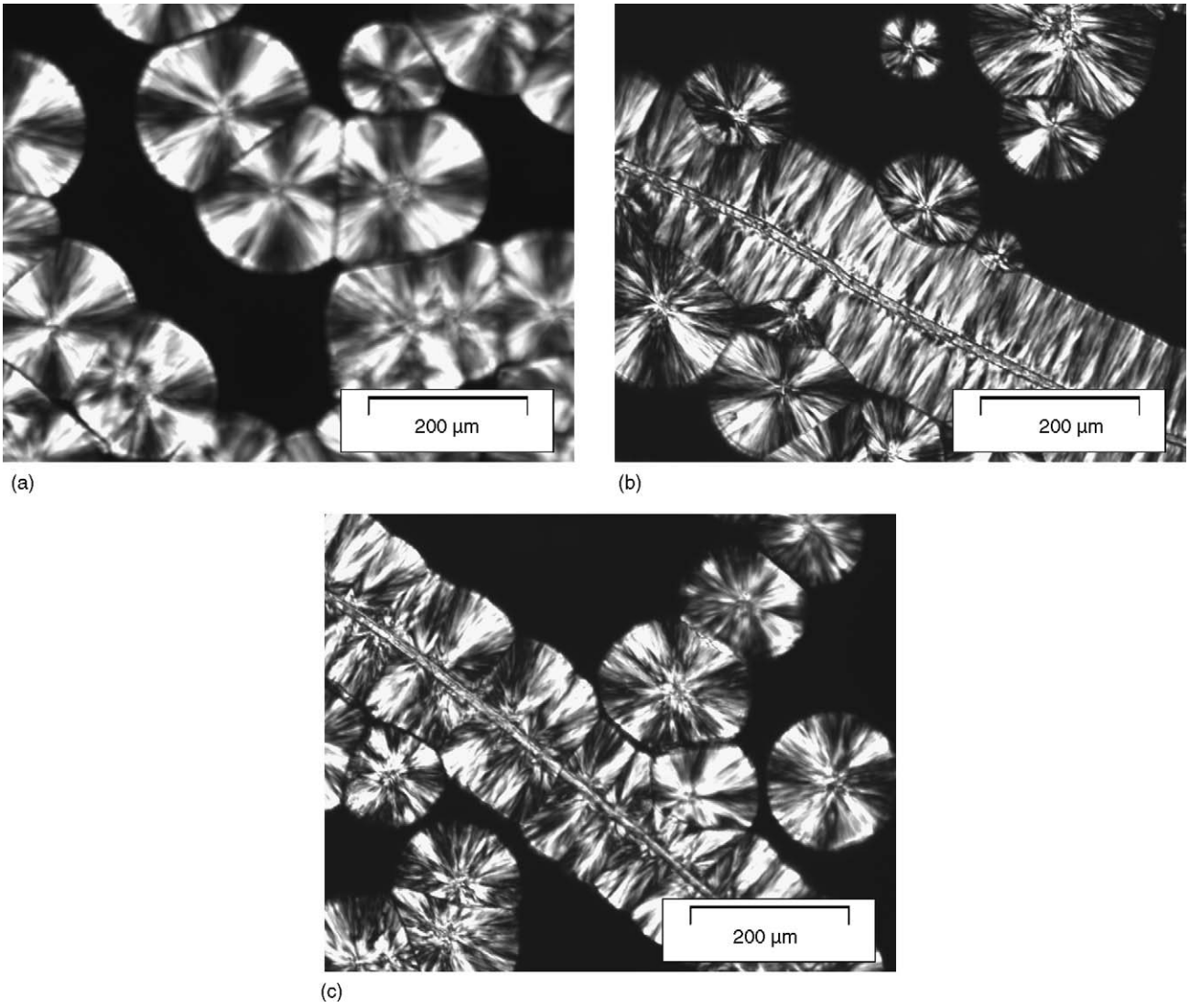

Fig. 7. Polarized optical micrographs of crystal growth of different samples after 50 min at 134 °C: (a) neat PP, (b) untreated flax + PP and (c) MAPP-treated flax + PP.

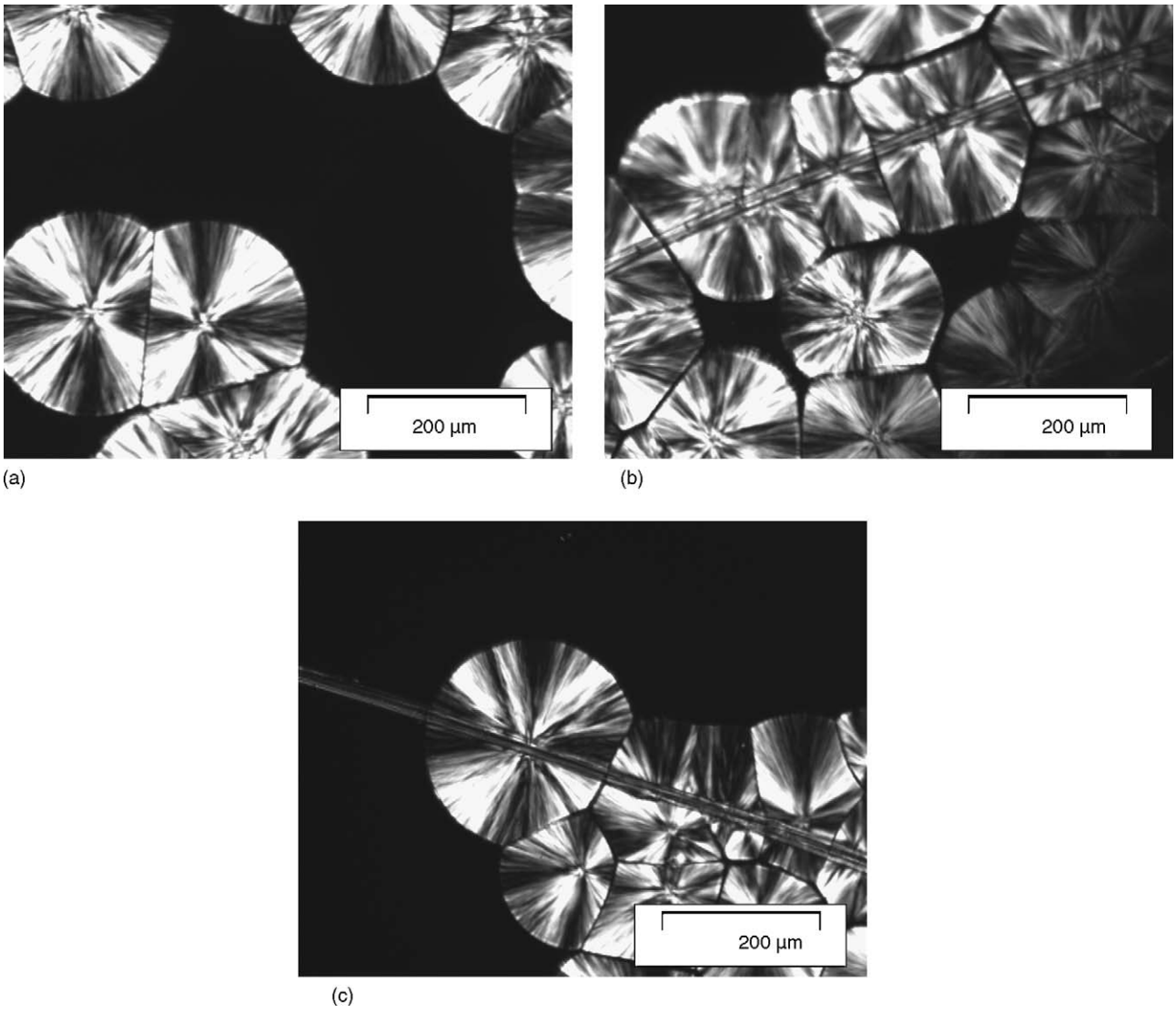

Fig. 8. Polarized optical micrographs of crystal growth of different samples after 204 min at 140 °C: (a) neat PP, (b) untreated flax + PP and (c) MAPP-treated flax + PP.

Transcrytallization (TC) is possible if the energetic conditions of nucleation are more favourable on the fibre surface than in the bulk of the melt [33]. The growth of TC proceeds perpendicularly to the fibre until the growing front impinges with spherulites nucleated in the bulk [50]. The mechanism by which TC layers occur is not fully understood and there are no rules to predict the appearance of TC in a particular fibre/matrix system. Besides, its effect on the properties of composites and on interfaces remains controversial [50]. The ability of different cellulose based fibres to induce transcrystallinity in PP composites has been reported [23,40,47,51,52] in the literature.

Fig. 7a shows that the spherulitic morphology produces a characteristic "Maltese cross", i.e. dark cross through the centre of the spherulite with wings in the direction of the planes of the analyzer and of the polarizer [33]. Fig. 7b and c shows polarized light microscope micrographs of a single flax fibre embedded in molten PP. At high super cooling values (Fig. 7b and c), untreated and MAPP-treated flax fibres act as nucleating agent for PP as nucleation occurs preferentially along the fibre axes. Thickness of the TC layer increases with time. The TC layer is not symmetrically developed around the fibre which is in agreement with the results obtained by other authors [47]. Besides, the nucleation density on untreated fibre surface is higher than on MAPP-treated fibre one. Fig. 8a–c shows the isothermal crystallization at 140 °C for neat PP, untreated and MAPP-treated polypropylene composites, respectively. While untreated fibre has active surface which induces transcrystallization, this is not observed in the case of MAPP-treated flax fibres. Therefore, crystal morphology in a fibre reinforced thermoplastic composite is strongly influenced by the surface treatment of fibres [42] but also by temperature. For PP–cellulose composites, it has been stated that pre-treatment with various chemicals of the cellulose surface inactivates the surface features responsible for nucleating the transcrystallinity [41]. Son et al. [52] expected that the coupling agent MAPP, which improves the interfacial interaction between cellulose and matrix, would be located at the interfacial region. According to this, it was expected that transcrystallinity would be inhibited or barely appeared by MAPP,

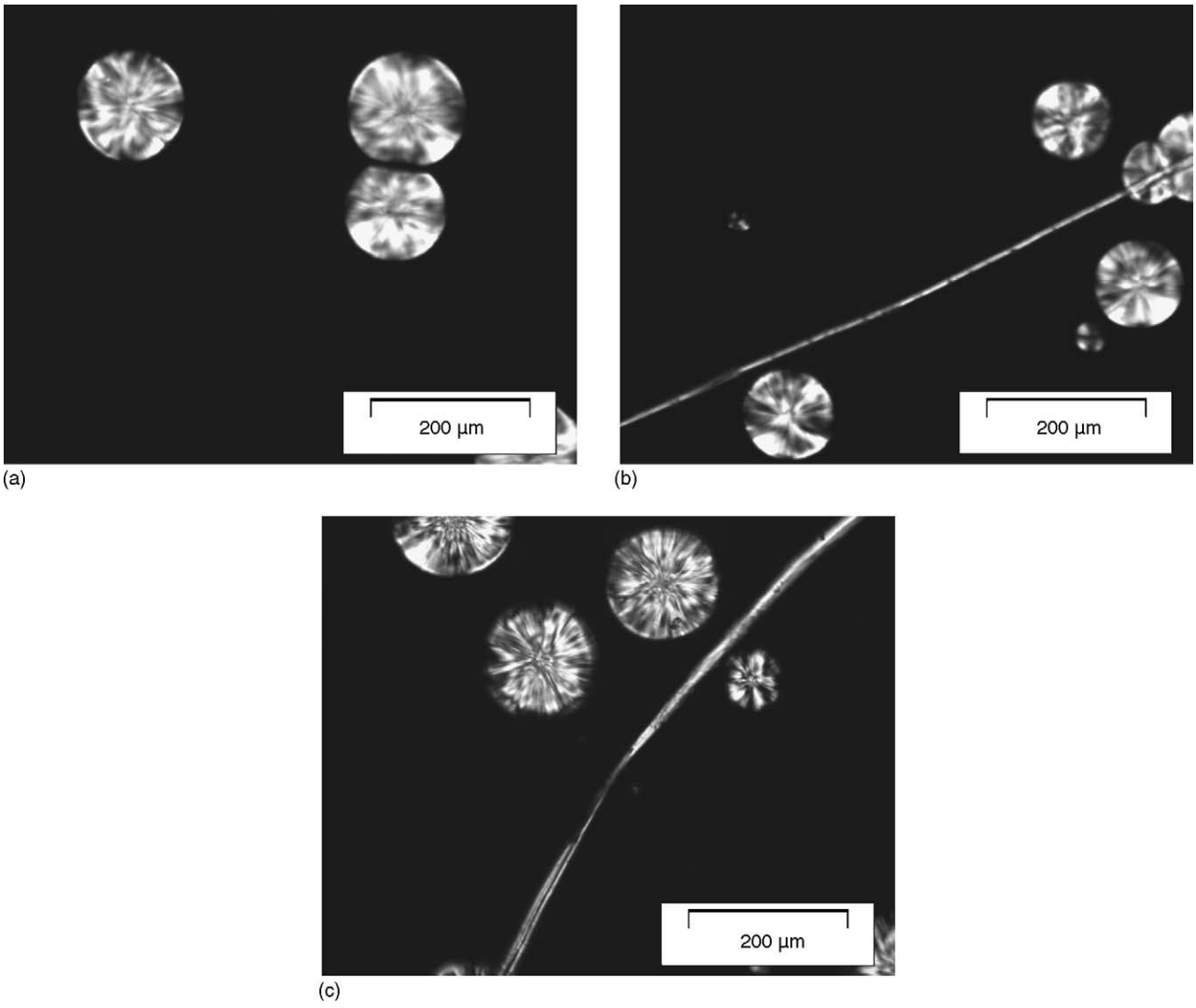

Fig. 9. Polarized optical micrographs of crystal growth of different samples after 144 min at 145 °C: (a) neat PP, (b) untreated flax + PP and (c) MAPP-treated flax + PP.

which is in agreement with Fig. 8c. For MAPP-treated fibres the density of nuclei in the transcrystalline layer was lower than for untreated flax fibre. This suggests that MAPP treatment modified the nucleation ability of flax fibre surface, thereby reducing the density of transcrystalline layer. As isothermal crystallization time increased, transcrystalline regions around fibre and spherulites in PP matrix propagated continuously. Their growth was terminated at certain time due to the impingement between them [52] and the matrix crystals. It can be seen that the number of nuclei increases initially as the temperature of crystallization decreases (Figs. 7b and 8b). Increasing supercooling, being the difference between the melting temperature of the matrix and the used isothermal crystallization temperature [53], the thickness of the transcrystalline layer decreased. The higher the crystallization temperature, the thicker the TC layer was. In addition to density of nuclei on flax surface decrease with increasing temperature, the formation of the TC layer became slower [47]. The nucleation density on both fibres and bulk decreased with increasing T_c [45], as shown in Figs. 7–9. Transcrystallization is strongly influenced by crystallization temperature and the increase in crystallization temperature reduced transcrystallinity [51]. At 145 °C (Fig. 9b and c) no transcrystalline layer was observed. Wagner et al. [54] showed that the number of active crystallization centres depends on the degree of supercooling.

4.5. Radii of spherulite and TC layer thickness

Fig. 10 shows the radii (r) of the biggest spherulites against growth time for different crystallization temperatures for neat PP. Initially, nice straight line is obtained for each temperature. As can be seen the values of r start to level off at later stage, the reason for this being growth is stopped by impingement of the spherulites.

Fig. 11 shows transcrystal thickness as a function of time at different crystallization temperatures for untreated flax fibre. Growth rate was linear and decreased with increasing crystallization temperature, which is in agreement with DSC and PVT data reported above. For talc/PP system, Naiki et al. [11] found

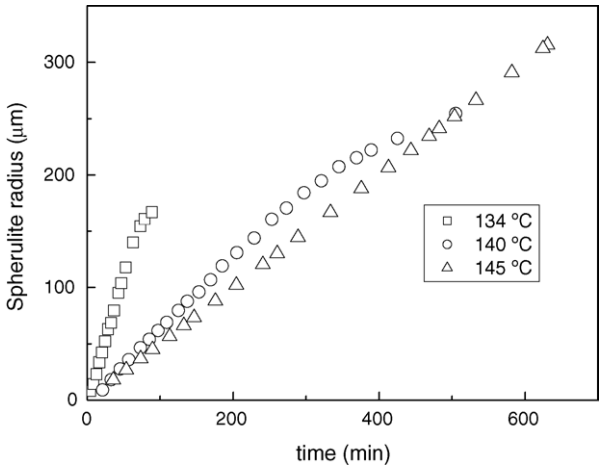

Fig. 10. Growth of polypropylene spherulite radii as a function of time under different crystallization temperatures.

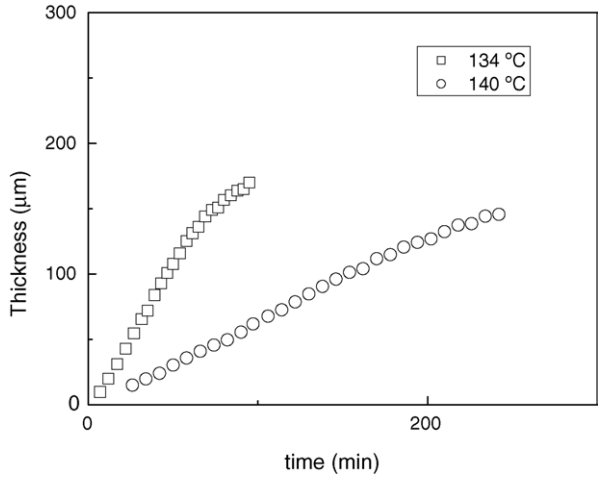

Fig. 11. Growth of the transcrystalline region from flax fibre as a function of time for untreated flax + PP composites under different crystallization temperatures.

that growth rate decreased with increasing crystallization temperature. The comparison of Figs. 10 and 11 shows that the radius of the spherulites is approximately equal to the thickness of the TC layer indicating that the crystallization at the fibre surface has started at almost the same time as the crystallization in the melt. It was clearly shown that the spherulite and transcrystal growth rate are equivalent, since the radius of the spherulite and thickness of the transcrystal are almost equal.

5. Conclusion

The effects of flax fibre surface modifications using maleic anhydride, maleic anhydride polypropylene copolymer, vinyltrimethoxy silane and alkalization, on fibre thermal stability and also on flax fibre/polypropylene composites crystallinity, have been investigated. TG analysis was carried out to study the thermal behaviour of untreated and treated flax fibres. Hygroscopicity of treated fibres decreased about 8–40% as a function of treatment used. Activation energy values calculated from Kissinger method for flax fibre main degradation step showed that treated fibres exhibit higher E values compared to untreated flax fibre ones. Avrami model used to describe polymer crystallization kinetics under isothermal conditions showed a good agreement between experimental and theoretical values for all systems. Isothermal crystallization was carried out in the temperature range of 134–145 °C by DSC and PVT measurements, and the values for Avrami exponent ranging from 2.34 to 2.89 and from 1.17 to 1.37, respectively, for PP were determined. For flax fibre/PP composites the Avrami exponent values obtained by DSC and PVT data were 2.18–2.89 and 1.17–1.54, respectively.

Calorimetric and volume measurements investigations showed that the incorporation of flax fibre in PP matrix causes an apparent increase in the crystallization rate. Besides, the crystallization rate is strongly influenced by crystallization temperature, fibre addition, fibre surface treatment and the pressure applied. The cooling rate from the melt to the crystallization temperature was found not to affect crystallization kinetics.

Optical microscopy results showed that the presence of flax fibres could lead to the development of transcrystallinity. The formation of transcrystalline structures is function of crystallization temperature and fibre surface treatment. The increase in crystallization temperature reduced the formation of transcrystallinity. MAPP-treated flax fibre composites showed lower transcrystalline density than composites with untreated fibres.

Acknowledgements

This research was performed as a part of the FP5 GROWTH-ECOFINA G5RD-CT1999-00147 Project in the framework of the Fifth European Research Program (www.ecofina.org). Financial support from the Diputacion Foral de Gipuzkoa is also gratefully acknowledged.

References

[1] N.E. Zafeiropoulos, C.A. Baillie, F.L. Matthews, Adv. Compos. Lett. 9 (2000) 291.
[2] G. Cantero, A. Arbelaiz, R. Llano-Ponte, I. Mondragon, Comp. Sci. Technol. 63 (2003) 1247.
[3] A. Arbelaiz, B. Fernández, G. Cantero, R. Llano-Ponte, A. Valea, I. Mondragon, Compos. Part A 36 (2005) 1637.
[4] N.E. Marcovich, M.M. Reboredo, M.I. Aranguren, J. Appl. Polym. Sci. 68 (1998) 2069.
[5] L.Y. Mwaikambo, E. Martuscelli, M. Avella, Polym. Test. 19 (2000) 905.
[6] P.R. Hornsby, E. Hinrichsen, K. Tarverdi, J. Mater. Sci. 32 (1997) 1009.
[7] B.V. Kokta, R.G. Raj, C. Daneault, Polym. Plast. Technol. Eng. 28 (1989) 247.
[8] K. Joseph, S. Thomas, C. Pavithran, Polymer 37 (1996) 5139.
[9] T.H.D. Sydenstricker, S. Mochnaz, S.C. Amico, Polym. Test. 22 (2003) 375.
[10] Y.S. Ismail, M.O.W. Richardson, R.H. Olley, J. Appl. Polym. Sci. 79 (2001) 1704.
[11] M. Naiki, Y. Fukui, T. Matsumura, T. Nomura, M. Matsuda, J. Appl. Polym. Sci. 79 (2001) 1693.
[12] A. Arbelaiz, G. Cantero, B. Fernández, I. Mondragon, P. Gañán, J.M. Kenny, Polym. Compos. 26 (2005) 324.
[13] L. Contat-Rodrigo, A. Ribes-Greus, R. Diaz-Calleja, J. Appl. Polym. Sci. 82 (2001) 2174.
[14] J.M. Stoddard, K.J. Shea, Thermochim. Acta 424 (2004) 149.

[15] A.K. Galwey, M.E. Brown, Thermal Decomposition of Ionic Solids, Elsevier, Amsterdam, 1999.
[16] M.G. Lu, M.J. Shim, S.W. Kim, J. Appl. Polym. Sci. 75 (2000) 1514.
[17] N. Regnier, S. Fontaine, J. Therm. Anal. Calorim. 64 (2001) 789.
[18] Eastman Chemical Company Data Sheet, Publication APG-1, September 1997.
[19] M. Kazayawoko, J.J. Balatinecz, R.T. Woodhams, J. Appl. Polym. Sci. 66 (1997) 1163.
[20] R.G. Raj, B.V. Kokta, J.D. Nizio, J. Appl. Polym. Sci. 45 (1992) 91.
[21] R. Karnani, M. Krishnan, R. Narayan, Polym. Eng. Sci. 37 (1997) 476.
[22] P. Gañan, I. Mondragon, Polym. Compos. 23 (2002) 383.
[23] P.V. Joseph, K. Joseph, S. Thomas, C.K.S. Pillai, V.S. Prasad, G. Groeninckx, M. Sarkissova, Compos. Part A 34 (2003) 253.
[24] K. Van de Velde, P. Kiekens, J. Appl. Polym. Sci. 83 (2002) 2634.
[25] P. Gañan, I. Mondragon, J. Therm. Anal. Calorim. 73 (2003) 783.
[26] P.R. Hornsby, E. Hinrichsen, K. Tarverdi, J. Mater. Sci. 32 (1997) 443.
[27] C. Albano, J. González, M. Ichazo, D. Kaiser, Polym. Degrad. Stab. 66 (1999) 179.
[28] K. Van de Velde, E. Baetens, Macromol. Mater. Eng. 286 (2001) 342.
[29] C. Devallencourt, J.M. Saiter, D. Capitaine, Polym. Degrad. Stab. 52 (1996) 327.
[30] Y. Mubarak, E.M.A. Harkin-Jones, P.J. Martin, M. Ahmad, Polymer 42 (2001) 3171.
[31] M. Avella, R. dell'Erba, E. Martuscelli, Polym. Compos. 17 (1996) 288.
[32] J.C. Hwang, C. Chen, H. Chen, W.O. Yang, Polymer 38 (1997) 4097.
[33] J. Karger-Kocsis, Polypropylene: Structure, Blends and Composites, vol. 1, Structure and Morphology, Chapman & Hall, London, 1995 (Chapter 3).
[34] C.Y. Kim, Y.C. Kim, S.C. Kim, Polym. Eng. Sci. 33 (1993) 1445.
[35] K. Cho, F. Li, J. Choi, Polymer 40 (1998) 1719.
[36] A. Amash, P. Zugenmaier, Polym. Bull. 40 (1998) 251.
[37] W. Qiu, F. Zhang, T. Endo, T. Hirotsu, J. Appl. Polym. Sci. 87 (2003) 337.
[38] M.A. Lopez Manchado, L. Torre, J.M. Kenny, J. Appl. Polym. Sci. 81 (2001) 1063.
[39] Y.S. Yadav, P.C. Jain, Polymer 27 (1986) 721.
[40] M. Avella, L. Casale, R. Dell'erba, B. Focher, E. Martuscelli, A. Marzetti, J. Appl. Polym. Sci. 68 (1998) 1077.
[41] A. Amash, P. Zugenmaier, Polymer 41 (2000) 1589.
[42] A. Kelly, C. Zweben, Comprehensive composite materials, Polymer Matrix Composites, vol. 2, Elsevier, Oxford, 2000 (Chapter 2.25).
[43] V. Ratta, Crystallization, morphology, thermal stability and adhesive properties of novel high performance semicrystalline polyimides, Ph.D. Thesis, Faculty of Virginia Polytechnic Institute and State University, 1999.
[44] K. Watanabe, T. Suzuki, Y. Masubuchi, T. Taniguchi, J. Takimoto, K. Koyama, Polymer 44 (2003) 5843.
[45] G. Bogoeva-Gaceva, A. Janevski, A. Grozdanov, J. Appl. Polym. Sci. 67 (1998) 395.
[46] J. He, P. Zoller, SPE ANTEC Tech. Pap. 37 (1991) 1723.
[47] N.E. Zafeiropoulos, C.A. Baillie, F.L. Matthews, Compos. Part A 32 (2001) 525.
[48] J.X. Li, W.L. Cheung, Polymer 40 (1999) 2085.
[49] S. Wong, R. Shanks, A. Hodzic, Macromol. Mater. Eng. 287 (2002) 647.
[50] H. Quan, Z. Li, M. Yang, R. Huang, Comp. Sci. Technol. 65 (2005) 999.
[51] J. George, S.K. Garkhail, B. Wieland, T. Peijs, Nat. Polym. Compos. (2000) 408.
[52] S. Son, Y. Lee, S. Im, J. Mater. Sci. 35 (2000) 5767.
[53] J. Loos, T. Schimanski, J. Hofman, T. Peijs, P.J. Lemstra, Polymer 42 (2001) 3827.
[54] H.D. Wagner, A. Lustiger, C.N. Marzinsky, R.R. Mueller, Comp. Sci. Technol. 48 (1993) 181.